MAX-lab
University of Lund
National Electron Accelerator Laboratory for
Nuclear Physics and Synchrotron Radiation Research

MAX publications (NTMX-7011) 1988

LUNTDX/(NTMX-7011)/1-17/(1988)

A 1.5 GeV HIGH BRILLIANCE SYNCHROTRON LIGHT SOURCE WITH COMBINED FUNCTION LATTICE.

M. Eriksson, L-J Lindgren, Å. Andersson, P. Röjsel and S. Werin

Postal Address:
Box 118
S-221 00 LUND, Sweden

Visiting Address:
Ole Römers väg 1

Telephone:
46-(0)46-107000
Telefax:

Telex:
33533 lunlvers

A 1.5 GeV HIGH BRILLIANCE SYNCHROTRON LIGHT SOURCE WITH COMBINED FUNCTION LATTICE.

Abstract.
A 1.5 GeV synchrotron light source with a combined function lattice is studied. The light source will offer X-ray radiation with $\lambda_c = 1.0$ Å from a superconducting wiggler and high brilliance VUV-radiation from undulators. The magnet lattice, magnet design and ring performance is discussed.

1. INTRODUCTION.

The first generation of SR-sources were synchrotrons with combined function lattices, i e the focusing quadrupole fields were integrated in the dipole bending magnets. The transverse beam dimensions were generally antidamped with large beam dimensions as a consequence. The second generation consists of separated function lattices, which means that separate dipoles, quadrupoles, etc are used. The third generation sources which are currently being built or planned (ALS, ESRF, TRIESTE, APS etc) have sophisticated separated function lattices which give very small beam emittances suitable for undulator operation.

When optimizing a third generation SR-source, several features must be observed. Since the off-momentum function must be kept small, we have to introduce a large number of magnet elements. To get positive chromaticity, we must use strong sextupoles where the off-momentum function is non-zero. This implies that the transverse dynamic aperture is reduced. This fact will generally limit the minimum emittance value and calls for additional sextupoles to hamper the resonance effects. Moreover, also the energy acceptance is limited since off-momentum particles will see a different lattice due to the focusing of the sextupoles.

Small emittance values can be achieved when using a combined function lattice [1)] . One can either use displaced quadrupoles or dipoles with a gradient. The damping rates can be controlled by choosing the bending radii in the magnets. If sextupole components are added to the combined function magnets, one can get quite large dynamical aperture and energy acceptance since the off-momentum particles will see an undisturbed lattice.

A simple combined function lattice is described below. The resulting emittance could easily be reduced to much smaller values if one chooses a larger circumference or accepts separate quadrupole magnets. The resulting ring has a 60 m circumference which is quite small compared to rings with similar performance.

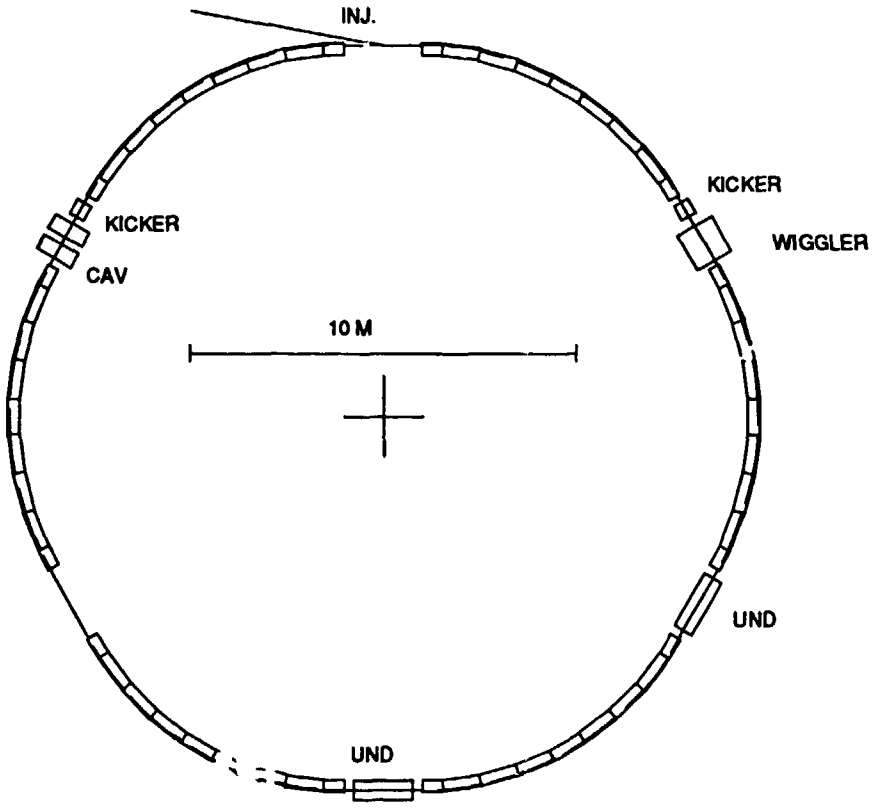

Fig 1. 1.5 GeV ring structure.

Table 1. Machine parameter values.

Max electron energy	1.5 GeV	
Circulating current	200 mA	
Hor emittance	1.2 10^{-8} rad m.	
Circumference	60 m	
Straight sections	6 * 2 m	
Critical wavelength		
	1.0 Å	Wiggler
	10, 20 Å	Bending magnets
RF	500 MHz	
Beam dimensions		
hor*vert (mm^2) FWHM	0.54 * 0.046	Straight section
	0.68 * 0.016	Bending magnet
Beam lifetime	7 h	

The ring is seen in fig 1 and the most important parameter values are seen in table 1.

2. MAGNET LATTICE.

2.1 BEAM OPTICS.

The machine functions for an elementary magnet cell are seen in fig 2. The next step is to introduce 2 m long straight sections between magnets consisting of eight elementary magnet cells. As seen in fig 3, the emittance is preserved while the vertical beta-function maximum amplitudes have grown. This lattice could do if we could accept the non-zero offmomentum function value in the straight sections. We do, however, plan for a strong superconducting wiggler which will increase the emittance value a factor 2.5. The final step will therefore be to adjust the lengths of the focusing magnets to get the off-momentum function value in the straight sections close to zero (fig 4). The emittance value will however increase due to the enlargement

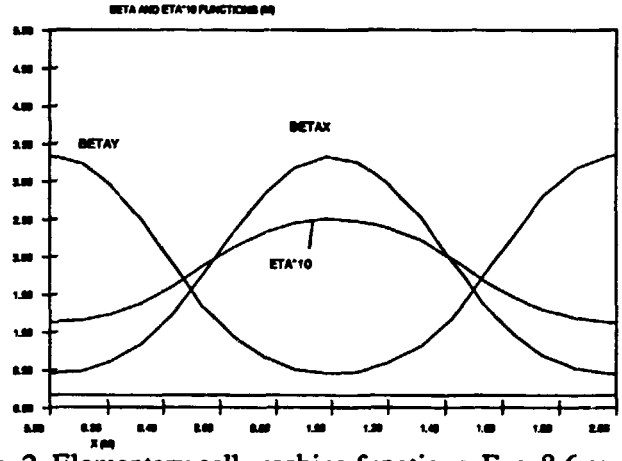

Fig. 2. Elementary cell machine functions. Em=8.6 exp -9

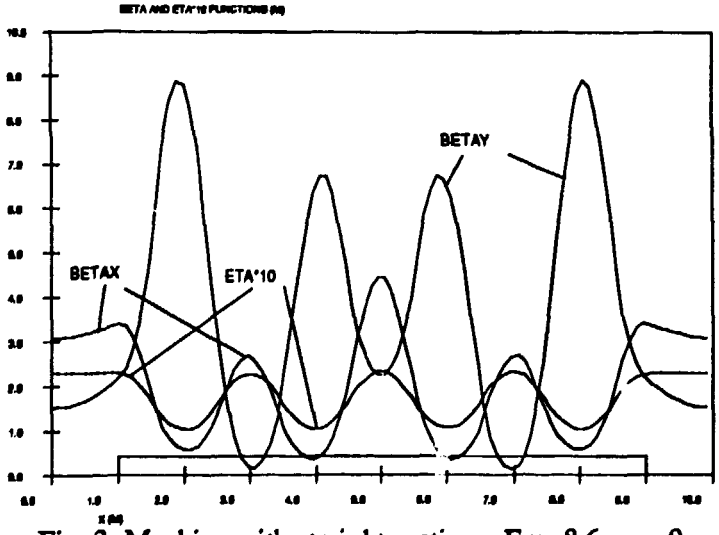

Fig. 3. Machine with straight sections. Em=8.6 exp -9

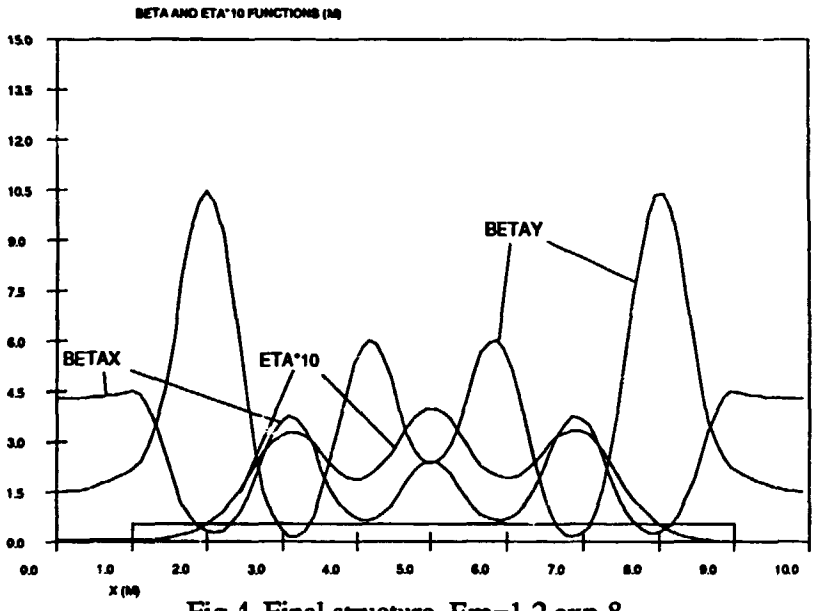

Fig 4. Final structure. Em=1.2 exp-8.

of the off-momentum function in the bending magnets.

The lattice design is quite flexible and the beam parameter values can be chosen differently. The dipole field can be reduced and the magnet length increased by 20% which will reduce the emittance a factor of two. Since our economical boundaries are quite tight, we will keep the 60 m ring circumference. The magnet parameter values for the proposed machine are seen in table 2.

Table 2. Magnet parameter values.

	Defocusing	Focusing
Length (m)	1.0	0.55, 0.9, 1.0
Bending radius (m)	5.73	11.46
Magnet field (T)	0.878	0.439
Gradient (T / m)	13.	13.
Sextupole comp (T/m^2)	52	30

2. 2. ALIGNMENT.

The proposed lattice provides a lot of focusing which demands pretty close tolerances for the alignment of the magnetic elements. The aligning tolerances are defined by the dynamic aperture, since we must have a stored beam before correcting the machine. For a safe injection and ramping without any need to correct the machine, except for the horizontal position at the injection septum at injection, we will ask for a maximum deviation of 3 mm in the ring.

Once the beam is trapped, we can measure the beam position. Correcting the lattice is not that critical until we have ramped to the operating energy. At this energy, however, a careful correction is necessary to get the assumed ratio between transverse emittances of 2.5 %, which will give us the high brilliance.

As mentioned above, the alignment tolerances are quite tight in this very strongfocusing lattice. The magnet design, however, with eight magnet cells mounted on the same girder, give us the possibility to position the magnet cells relative each other with a RMS error of 30 μ m.

The positioning of the long magnets, which form elementary cells, is not that crucial. In this case, a RMS positioning error of 0.1 mm will only give a negligible closed orbit error compared to the positioning error described above.

The closed orbit deviation for randomly displaced quadrupoles is given by

$$< x^2_{co}(s) > = \Sigma \beta(s)\ \beta_k\ (x'_k)^2 / (2 \sin(Qx\ \pi))^2$$

where $x'_k = \Delta k l / B\rho$ is the resulting kick and
Δ = quadrupole displacement
k = quadrupole strength
l = quadrupole length.

With the mamimum closed orbit deviation given above, we should align the magnet elements within 0.03 mm vertically and 0.075 mm horizontally (RMS).

If a whole magnet, being a unit cell, is misaligned a distance Δ, we will get a closed orbit error of

$$< x^2_{co}(s) > = \Delta^2 \beta(s) / \beta_\Delta$$

This effect will be masked by the misalignment of the magnet cells.

A magnet cell tilt of 0.03 mrad relative to the other magnet cells in one main magnet, a dipole field variation within 10^{-4} and a dipole length error of 0.1 mm give also a minor contribution to the closed orbit deviation.

2.3. CORRECTIONS.

The main reason to correct the machine is to reach a low emittance coupling and a small vertical dispersion. A perfect machine will have a vanishing vertical beam size, but emittance coupling and vertical dispersion will in fact define the vertical beam dimension and then also the photon brilliance.

2.3.1. VERTICAL DISPERSION.

The sources for the vertical dispersion are tilted dipoles (negligible), skew quadrupoles and closed orbit deviations in the sextupoles. (We here refer to the multipole components in the magnet elements.)

A skew quadrupole which is rotated an angle α, will have an radial magnet field component

$B_x = \alpha\, k\, x.$

If we have a radial dispersion η_x at the skew quadrupole, we will get

$x = \eta_x\, \delta$, where $\delta = \Delta p / p$.

The radial magnet field will then give a vertical kick, which will result in a vertical dispersion

$\eta_y = \beta_y\, \alpha\, k\, \eta_x\, l / (B\, \rho\, 2 \sin(Q_y\, \pi))$

With the alignment tolerances given above, skew quadrupoles will give a vertical dispersion of 1.6 mm, which is a very small value.

A particle with an closed orbit offset in a sextupole will see a radial magnet field

$B_x = q\, x\, y_{co}$ where q is the sextupole strength.

With the same reasoning as above, we will get

$\eta_y = \beta_y\, l\, q\, \eta_x\, y_{co} / (B\, \rho\, 2 \sin(Q_y\, \pi))$

The uncorrected machine will give a maximum vertical dispersion of 0.2 m, which with an energy spread of $0.6\ 10^{-3}$ will give a much to large vertical beam size.

2. 3. 2. COUPLING.

The coupling mechanism between the oscillations in the transverse directions is similar to the dispersion effect described above. In our case, the vertical closed orbit deviation effect in the sextupoles is dominant compared to skewed quadrupoles similarly to the dispersion effect. We will end up with a coupling for one sextupole element

$\kappa_{el} = q\, l\, y_{co}\, (\beta x\, \beta y)^{1/2} / (4\pi\, B\, \rho)$.

Summed over all elements, we get the vertical emittance

$\varepsilon_y = \varepsilon_x\, (\kappa / \Delta)^2 / ((\kappa/\Delta)^2 + 0.5)$ where Δ is distance between the tunes.

With $\Delta = 0.05$, we must have $\kappa = 0.005$ or smaller to get the specified emittance coupling. The uncorrected machine gives us $\kappa = 0.025$, which is quite unsatisfactory. The correcting and diagnostic alements must be able to adjust the machine to an vertical error of 0.6 mm if we should achieve the low emittance coupling.

2.4. CORRECTING ELEMENTS.

As seen above, the beam position in the vertical direction is the most crucial one at full energy. For a careful adjustment we need a total of 24 vertical correcting coils wound around the magnet mirrors in the focusing magnets (Fig 6.).

The radially correcting elements are somewhat more complicated. It can be discussed wether they in fact are necessary judging from the discussion above. It seems however, a bit too radical to omitt these correction. We can introduce backleg windings in the magnet cells for this purpose. These corrections will also influence the gradients in the magnets. This effect is however small and the tunes can be brought back with the gradient correction. The question wether the radial corrections can be omitted and if not, the design of them will be studied in more detail.

We also need corrections at injection. Dipole corrections at the kicker magnet positions is a natural choice.

3. MAGNET DESIGN.

All main magnets have dipole, quadrupole and sextupole components. The magnets and their fields are seen in fig 5-6.The magnet cells in a main magnet have a common girder and a common coil. The magnet cells are separated by small gaps to cut off the longitudinal magnet fields. These gaps should eventually be enlarged with some 10 cm to allow for correcting elements.

Although the magnets will be ramped after injection, solid steel will be used in the magnets due to the strict magnet tolerances. Pole face windings will be used for gradient corrections, alternatively, short correcting quadrupoles can be introduced between the magnet cells.

The general idea when designing the magnets was to construct a half quadrupole with a steel plate to cut off the magnet field in the vertical midplane. This idea works nicely in the focusing

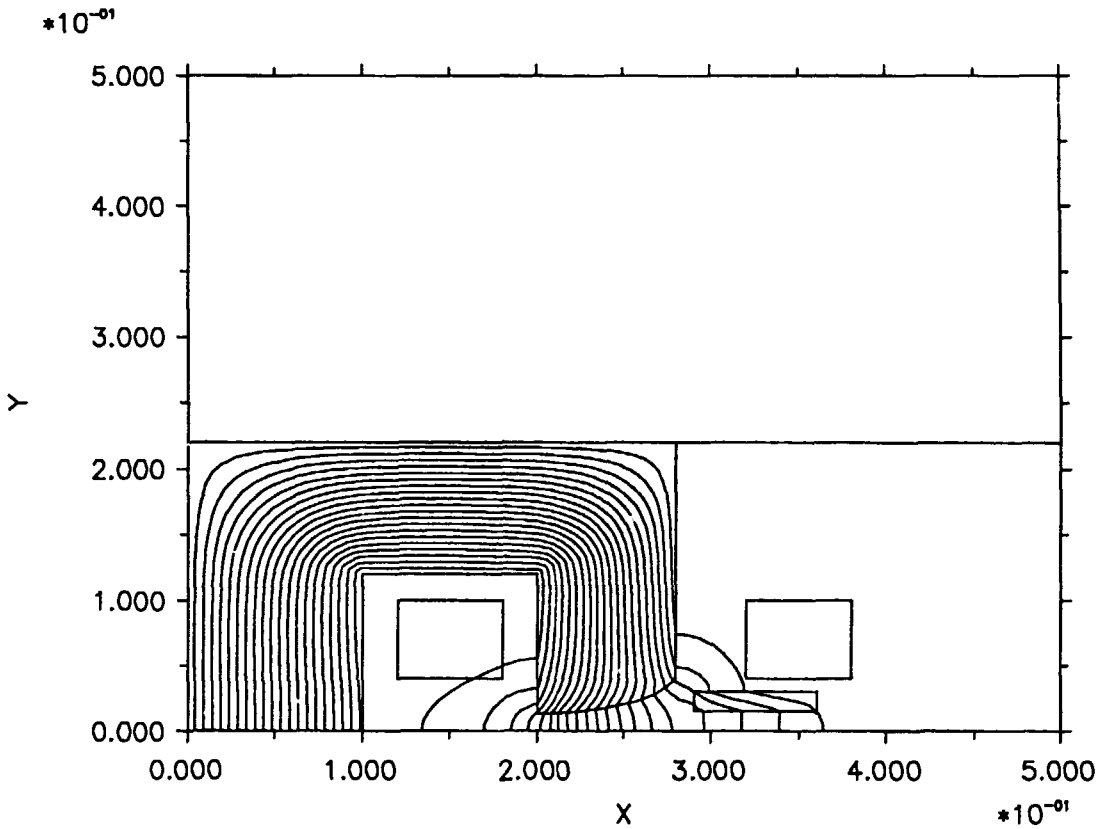

Fig 5a. Defocusing magnet cell.

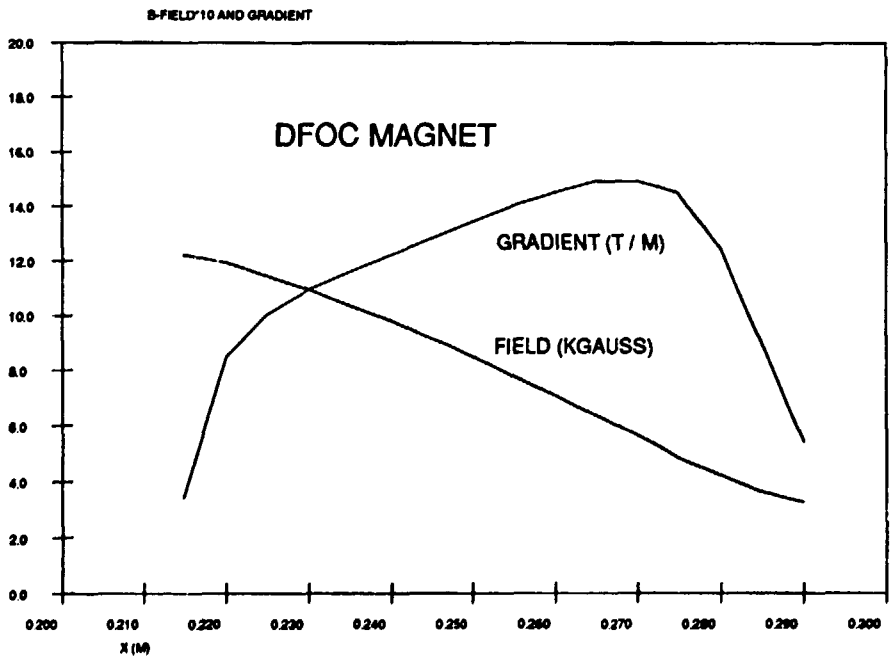

Fig 5b. Field and gradient in dfoc magnet cell

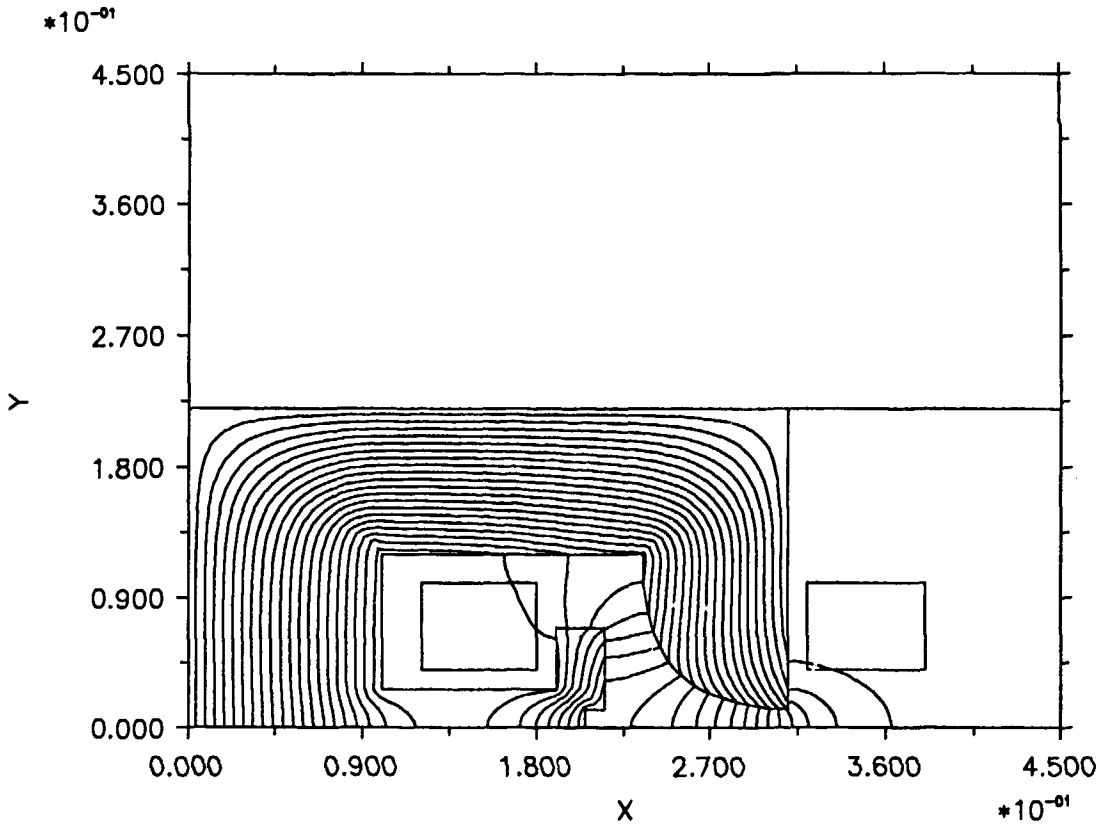

Fig 6a. Focusing magnet cell.

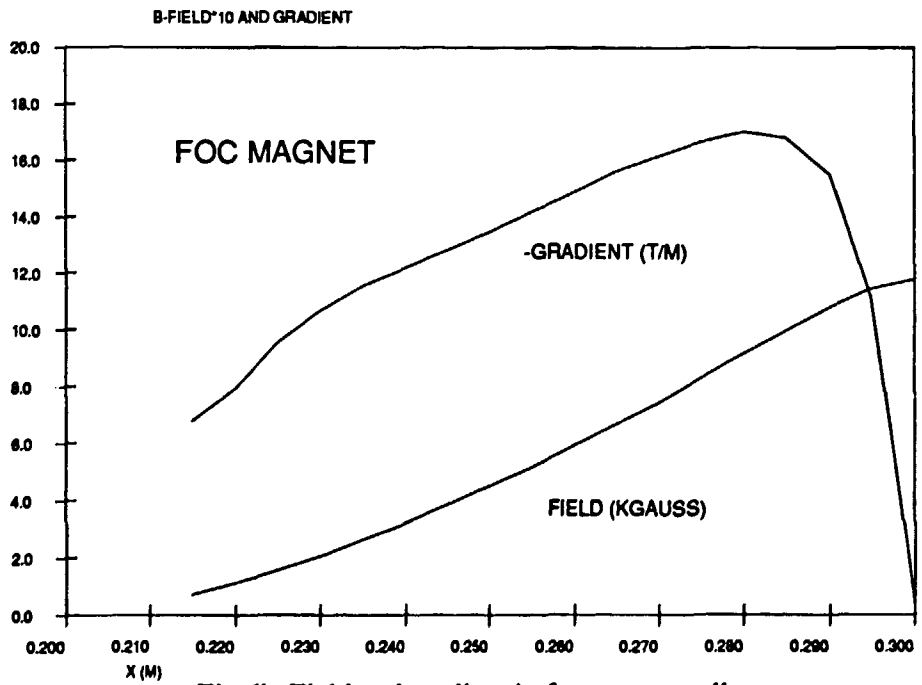

Fig 6b. Field and gradient in foc magnet cell.

magnet case. We have a cut in the steel to allow for the vacuum chamber inwards the magnet. In the defocusing case however, we must allow space for the light beamlines. Steel plates are therefore introduced above and under the median plane to lower the magnet potential there.

4. INJECTION.

Two accelerators are available as injectors at MAX, one 100 MeV racetrack microtron and one 550 MeV storage ring [2].

The intrabeam scattering process (IBS) is quite pronounced at 100 MeV in the 1.5 GeV ring due to the long damping times. Since the beam dimensions then are pretty large, we do not foresee any self-clearing of trapped ions due to overfocusing. When accelerating the beam after stacking, the beam will shrink in the transverse directions since the damping times decrease strongly. The trapped ions will then give a betatron tune spread given by the increased focusing by the trapped ions. The maximum current which can be accelerated from 100 MeV is estimated to be 50-100 mA judging from experiments at the present MAX storage ring.

At 500 MeV, the IBS is still present and dominates the emittance value, but this is small enough to allow for self-clearing of the ions. The injection rate, on the other hand, is quite low due to the slow-cycling 550 MeV ring, and this will make the adjustment of the ring difficult. Moreover, one might get difficulties to get circulating currents which are high enough for the conditioning of the vacuum tank when the gas scattering lifetime is short in the unconditioned machine.

We will therefore start to inject at 100 MeV from the racetrack microtron using the fast-stacking method developed at the existing ring [3]. The pulse from the microtron can easily be observed in the ring by the TV-monitors. Once the beam is trapped, a couple of mA is enough to adjust the machine at all energies. A preconditioning can then take place with a circulating current of 50-100 mA and the first synchrotron light experiments can start simultaneosly.

Once the ring is adjusted at 500 MeV and preconditioned, we can inject from the existing storage ring.

The injection items are quite conventional. A pulsed septum magnet will inflect the injected beam in the horizontal phase space. Two kicker magnets placed 1.25 betatron wavelengths from the injection point (in the adjacent straight sections) will move the closed orbit at the injection moment.

5. RF SYSTEM.

The same RF as used in the present MAX ring will also be used in the 1.5 GeV ring. The total voltage needed to get a sufficient Touschek lifetime is 0.8 MV. We will then use two cavity cells fed by a 100 kW klystron. The RF-parameters are seen below.

RF	500 MHz	
Nr of cells	2	
Cell shunt impedance	7M Ω	($P=U^2/R_{sh}$)
RF voltage	0.8 MV	
Klystron power	100 kW	

A passive 1500 MHz Landau cavity system, similar to the one used in the present MAX ring [4], will also be used to kill the longitudinal coupled bunch oscillations.

6. DIAGNOSTICS.

The beam monitoring system must cope with the demand to correct the beam within 0.6 mm. Similar diagnostic systems as the ones used at the present MAX ring will be used. The main diagnostic device is the CCD-camera with which both beam profiles and positions can be measured with a precision down to 30 μm. The synchrotron light used for the CCD-cameras will be taken out from the ring via watercooled steel mirrors.

The betatron tunes will be measured by a spectrum analyzer connected to a pair of striplines in the vacuumchamber and a tracking generator connected to an excitation coil.

For the measurement of the circulating current, a DCCT will be used.

7. VACUUM SYSTEM.

Most of the ring circumference is covered by the magnets. The minimum gap height is 25 mm, which will give us 20 mm height inside the vacuum chamber. No in situ baking equipment will be used. The main pumping will be made by discrete ion pumps outside the magnets. The vacuum system is designed to allow for currents up to 400 mA, which is twice the expected operating current.

Each main vacuum chamber will be eight m long and made of stainless steel segments. A 20 mm high vacuum chamber is placed inside the dipole magnets and connected to a tube 100 mm in diameter as seen in fig 7. The tube is slotted towards the beam vacuum chamber to allow for pumping and to transmit the synchrotron radiation which will hit the heat absorbers placed in the tube. Some 10 % of the radiation will hit the remaining wall between the slots in the tube. Since

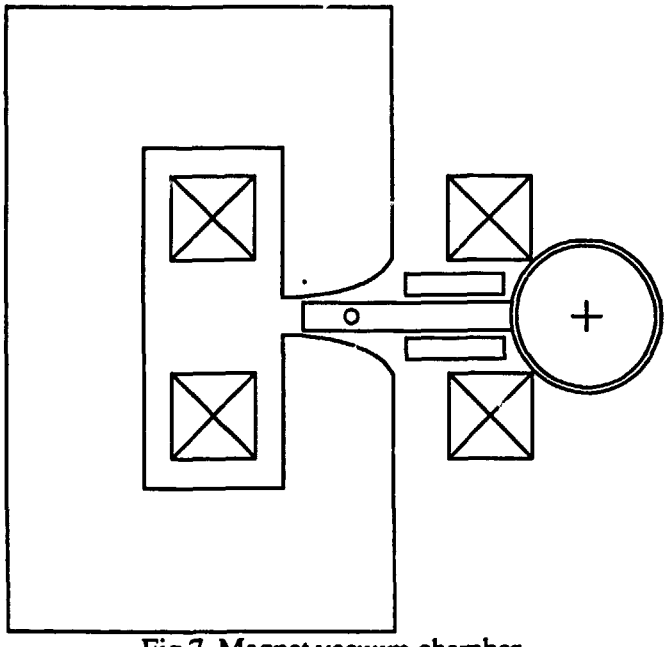

Fig 7. Magnet vacuum chamber.

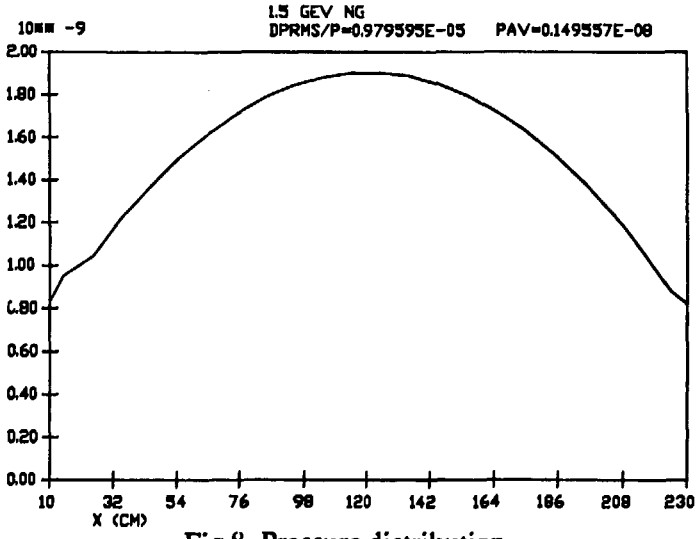

Fig 8. Pressure distribution.

the bending radius in the dipoles is rather large, the radiating power is only 3.6 W/mrad at a circulating current of 400 mA. The most critical spot in the tube support is the area facing the radiation. At this local spot, $0.3*4$ mm ^{2} in size, will get a temperature rise of $300\ ^0$ C at 400 mA , which is quite acceptable.

The power density level at the wiggler beamport is however a factor of ten higher. The tube supports must be shielded here with watercooled copper absorbers. Since the thermal conductivity is a factor of twenty higher in copper compared to stainless steel, the temperature increment at the critical spots of these absorbers will be some $150\ ^0$ C.

The heat absorbers in the tube outside the beam vacuum chamber are constructed as watercooled copper fingers which are struck perpendicularly by the radiation to give minimum gas emission yield.

The tube outside the beam vacuum chambers fills two functions. First, the large conductance will make efficient use of the pumps. An optimum design where the pressure raises to the double value in the mid between the pumps will be achieved if 500 l/s pumps are placed every second m around the magnet. The second feature is that the narrow beam vacuum chamber will be drained on its RF-fields, which will lower the vacuum chamber impedance.

The pressure needed to get a lifetime matching the Touschek lifetime is about 5 nTorr (see below). The calculated mean pressure including beamloading is 1.5 nTorr with the design described above, which means that the gas scattering effect will not define the beam lifetime.

8. BEAM DYNAMICS.

8.1 DYNAMICAL APERTURE.

Since the sextupole components are integrated in the focusing elements, the energy acceptance is quite high. The dynamical aperture calculated by trackin particles is seen in table 3. The beam amplitudes are given at the position of the maximum beta function values. It is seen from table 3 that the vacuum chamber is matched to the dynamical aperture.

Table 3. Dynamical aperture.

Radial	20 mm
Axial	10 mm
Energy acceptance	10 %

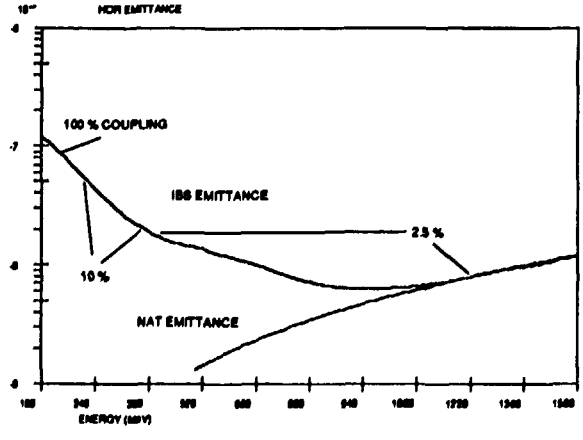

Fig 9. Emittance (IBS)

8.2 INTRA-BEAM SCATTERING.

At a low-emittance ring as the one proposed, IBS is quite pronounced at lower energies. This is however not of any larger disadvantage in itself since we only intend to inject and ramp at the lower energies. On the contrary, IBS will provide us with a sufficiently large beam to get a long Touschek life time. The main disadvantage is that we will get ion trapping below 500 MeV.

The IBS effect on the beam is calculated with the code ZAP [5] at different energies for a

circulating current of 200 mA. The result is shown in fig 9. Some assumptions have been made for the calculations:

1. The coupling is assumed to be 2.5 % for energies from 300 MeV and above. The reason for this is that we assume selfclearing of the ions at these energies. At lower energies, this is not the case and full coupling is assumed at 100 MeV and 10% at 200 MeV.

2. The RF voltage is 0.8 MV at energies from 300 MeV and above. At lower energies, the RF voltage is reduced.

8.3 BUNCH LENGTHENING.

Since the momentum compaction factor is rather high, this machine can accept quite a high vacuum chamber impedance and still have the natural bunchlength in the multi-bunch mode at high energies. On the other hand, the vacuum-chamber impedance is rather high due to the small vacuum-chamber gap. The vacuum-chamber impedance is assumed to be 20 Ω.

At lower energies, the bunchlengthening will be masked by the IBS effect.

8.4 BEAM LIFE-TIME.

The gas pressure is assumed to be 1.5 nTorr in the conditioned machine. The vacuum-limited life-time is then 26 h at full energy .The main limiting effect is the bremsstrahlung loss, which give a life-time of 37 h. The aperture dependent gas-scattering lifetime is 90 h, which means that the vacuum chamber dimensions have little influence on the life-time.

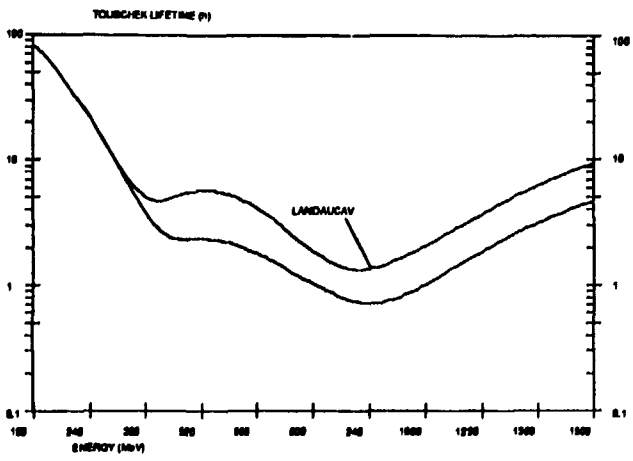

Fig 10. Touschek lifetime.

The major life-time limitation is the Touschek effect. The Touschek lifetime is seen in fig 10. At 1.5 GeV, the Touschek lifetime is 5 h and decreases with decreasing energy until the intrabeam scattering increases the beam dimensions. The Touschek lifetime in the energy region between 200-500 MeV is difficult to calculate exactly, since the coupling is depending of the ion neutalisation of the beam. We know, however, that we will have full coupling at 100 MeV and prefer to use a pessemistic assumption of low coupling at higher energies. Again, the RF voltage is 0.8 MV or matched to the dynamical aperture at lower energies.

The 1.5 GeV machine will be operated with the Landau cavity to avoid energy blow-up above 1 GeV. The bunch length will then be increased a factor of two and so will the Touschek lifetime. This is seen in the upper curve in fig 10.

8.5 ION TRAPPING.

Ion trapping is a serious obstacle in especially low energy electron rings like the present MAX ring. These ions, created by the ionization of the restgas by the electron beam, is trapped by the negative electron beam and will then influence the focusing of this beam by its space charge. For sufficiently high electron densities, the ion oscillation frequency will be high enough so a gap in the electron beam will create overfocusing of the ions which then will leave the electron beam. This condition will met at energies above 300 MeV in the 1.5 GeV ring.

At 100 MeV, however, the IBS will enlarge the beam that much so the necessary gap in the electron beam to create ion overfocusing is unrealistically large. This means that we might get problems to stack currents higher than some ten mA if no additional ion-clearing is introduced. This will especially be critical at the commissioning of the ring before the proper vacuum is attained.

If an ion is created in a straight section, it will propagate along the beam with thermal velocity. When reaching the dipole magnets, it will be reflected backwards [6] ; the dipoles are acting like isolators. If an ion is created in a dipole field, the ion will be accelerated by the cross-fields of the magnet field and the electron beam electric field. In our case, the ion kinetic energy is typically 10 eV.

Most of the proposed ring (80 %) is covered with dipole magnets. Ions created in these dipoles will travel along the machine at rather high speeds, typically 3 km/s. Due to this relatively high speed, it will be sufficient to introduce clearing electrodes of proper length in some of the straight sections.

9. RADIATION CHARACTERISTICS.

One major aim with this ring is to provide X-ray radiation from high-field wigglers. The first one is the 8 T wiggler currently being built at TTH, Finland and we take its parameter values when calculating the emitted radiation at a beam energy of 1.5 GeV.

The undulator case is from the undulator being built by VTT, Finland, where the first MAX undulator [7] was built and an undulator with longer magnet period. The undulator parameter values are seen below.

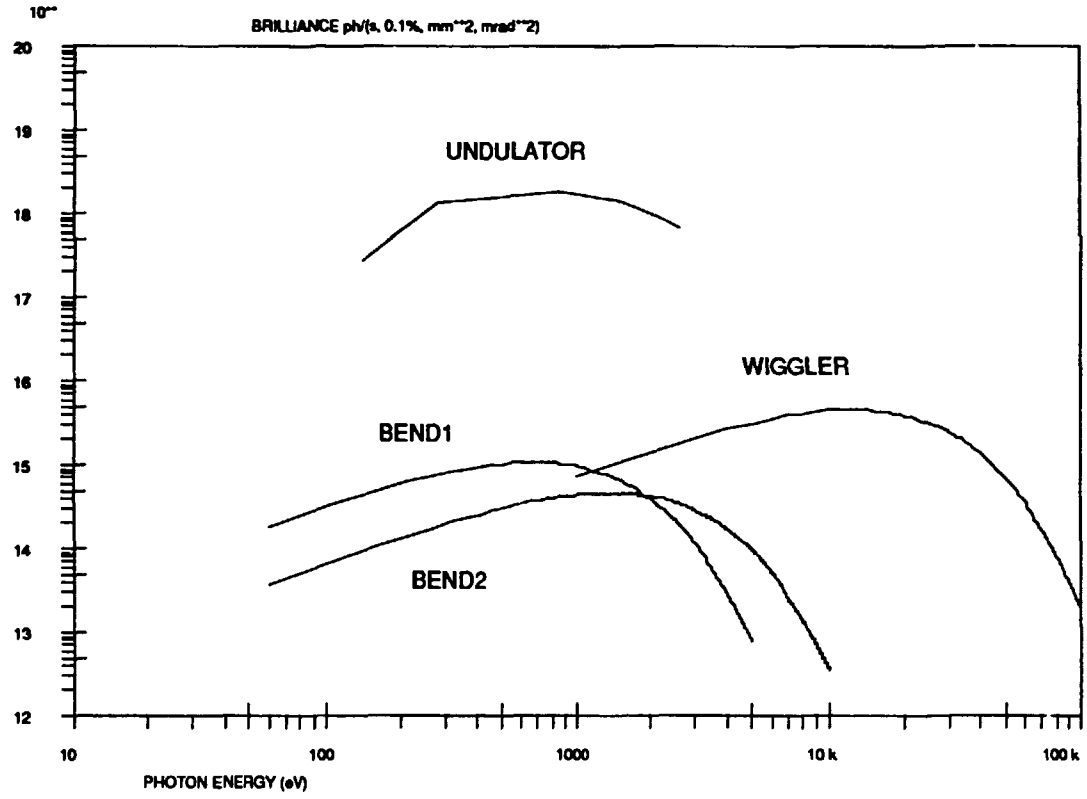

Fig 11. Brilliance.

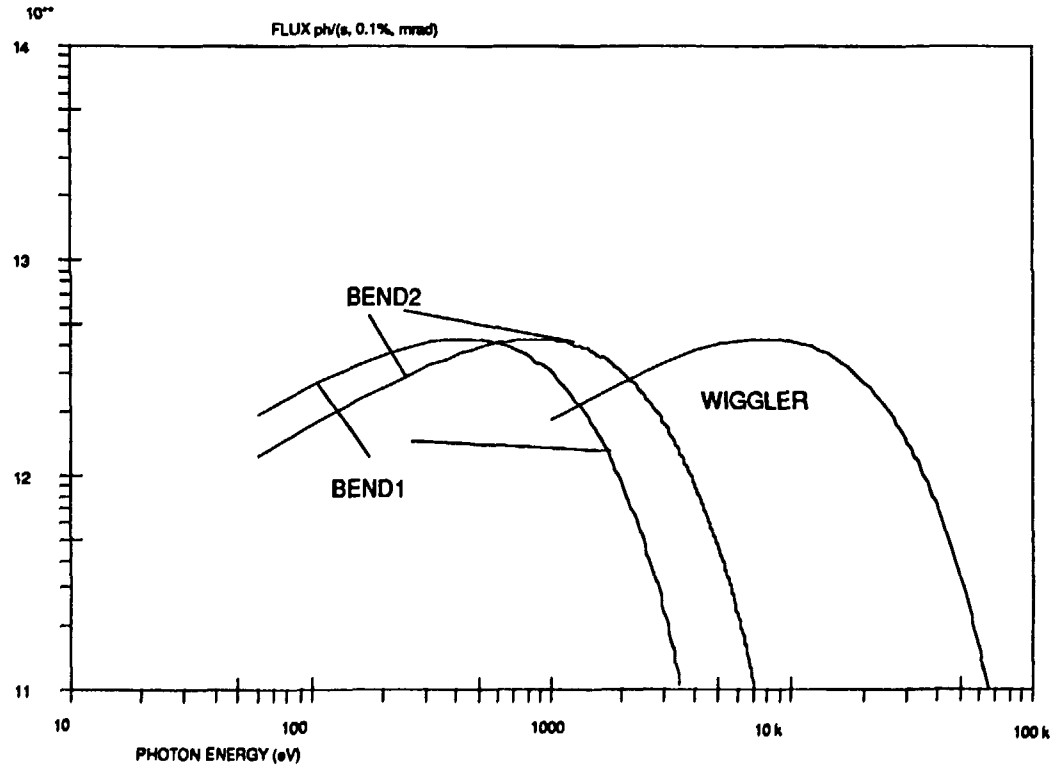

Fig 12. Flux.

Table 4. Undulator parameters.

Magnet period (cm)	2.4	5.
K	0-2	0-2
N	60	30

Rather high harmonics, as in the case of the present MAX ring are used when calculating the brilliance spectra.

We also assume that the ring will be operated at 1.5 GeV. If we want to decrease the lower energy limit for the undulator radiation, it is possible to decrease the electron energy.

The relatively short straight section length is sufficient for the two cases described above. It does not pay off that much to increase the number of undulator periods regarding the difficulties which the tightening of the undulator tolerances will imply and the fact that the electron beam emittance will become dominating. The proposed undulator will cover the energy region 100-3000 eV. For lower photon energies, the present MAX ring will cover the 10-150 eV range.

The brilliance and flux for the proposed ring is seen in fig 11 and 12. The high brilliance from the wiggler and especially from the undulator reflects the small beam emittance.

References:

1. W. D. Klotz and G. Muhlhaupt, A Novel Low Emittance Lattice For High Brilliance Electron Beams. To be published in Nucl. Instr. and Meth.

2. M. Eriksson, The Accelerator System MAX, Nucl. Instr. and Meth. 196 (1982) 331.

3. L.-J. Lindgren. Fast Stacking At Low Energy Injection, to be published.

4. MAX-lab Activity Report 1987.

5. M. S. Zisman, S. Chattopadhyay and J. J. Bisognano, ZAP, LBL/21270 UC-28.

6. CERN Accelerator Scool, CERN 85-19.

7. M. Eriksson, T. Meinander and S. Werin, A VUV Undulator For MAX, Nucl. Instr. and Meth, A265, (1988) 587-595.

ISSN 0284-1258